

Photodynamic Therapy Mediated by Aloe-Emodin Inhibited Angiogenesis and Cell Metastasis Through Activating MAPK Signaling Pathway on HUVECs

Technology in Cancer Research & Treatment
Volume 17: 1-11
© The Author(s) 2018
Article reuse guidelines:
sagepub.com/journals-permissions
DOI: 10.1177/1533033818785512
journals.sagepub.com/home/tct


Qing Chen, MD¹, Kai-Ting Li, MD¹, Si Tian, MD¹, Ting-He Yu, PhD²,
Le-Hu Yu, PhD³, Hai-Dan Lin, MD¹, and Ding-Qun Bai, PhD¹ 

Abstract

Photodynamic therapy is a clinically used, minimally invasive therapeutic procedure that involves the application of photosensitizers which can locate in target cells and so be irradiated at a corresponding wavelength. Laser light irradiation activation of photosensitizers generates free reactive oxygen species, which induces selective cytotoxic activity in target cells. Within recent years, aloe-emodin as a photosensitizer has been successfully applied in photodynamic therapy applications. Angiogenesis plays an important role in tumor growth and metastasis; thus, the development of a novel target treatment for angiogenesis is essential in order to improve treatment therapeutics for cancer treatment. An essential step in angiogenesis involves the formation of tube-like structures during matrix degradation, rearrangement, and apoptosis of endothelial cells. In the present study, we investigated the mechanisms of photocytotoxicity induced by aloe-emodin in human umbilical vein endothelial cells. Analysis of cell proliferation results noted a significant decrease in cultured cells which received various concentrations of aloe-emodin and photodynamic therapy-induced light doses. Additionally, mitochondrial mechanisms of apoptotic cell death were observed in aloe-emodin photodynamic therapy-treated cells, as tube formation assays noted angiogenesis suppression after treatment. The capacity of migration and invasion of human umbilical vein endothelial cells was measured using the transwell assay and demonstrated that aloe-emodin photodynamic therapy significantly inhibited the migration and invasion of human umbilical vein endothelial cells. The expression of p38, extracellular signal-regulated kinase, the c-Jun N-terminal kinases, and vascular endothelial growth factor suggested that the cellular metastasis was related to mitogen-activated protein kinase signal pathway. Furthermore, disorganization of F-actin cytoskeleton components was observed after aloe-emodin photodynamic therapy. Overall, the findings from this study suggest that aloe-emodin photodynamic therapy inhibited angiogenesis and cellular metastasis in human umbilical vein endothelial cells by activating the mitogen-activated protein kinase apoptotic signaling cell death pathway.

Keywords

aloe-emodin, MAPK signal pathway, photodynamic therapy, angiogenesis

Abbreviations

AE, aloe-emodin; EdU, 5-ethynyl-2-deoxyuridine; ERK, extracellular signal-regulated kinase; HUVEC, human umbilical vein endothelial cell; JNK, the c-Jun N-terminal kinases; MAPK, mitogen-activated protein kinases; PA, paraformaldehyde; PBS, phosphate-buffered saline; PDT, photodynamic therapy; PS, photosensitizer; ROS, reactive oxygen species; VEGF, vascular endothelial growth factor.

Received: September 27, 2017; Revised: March 28, 2018; Accepted: May 31, 2018.

¹ Department of Rehabilitation, The First Affiliated Hospital of Chongqing Medical University, Chongqing, China

² Department of Gynaecology and Obstetrics, The Second Affiliated Hospital of Chongqing Medical University, Chongqing, China

³ Department of Rehabilitation, The Second Affiliated Hospital of Chongqing Medical University, Chongqing, China

Corresponding Authors:

Ding-Qun Bai, PhD and Hai-Dan Lin, MD, Department of Rehabilitation, The First Affiliated Hospital of Chongqing Medical University, Chongqing, China.
Emails: baidingqun@163.com, hopelam@126.com



Introduction

Photodynamic therapy (PDT) is a new treatment that is minimally invasive and exerts selective cytotoxicity for target cells. Study showed cancers of skin, bladder, lung, esophagus, and cervix can be managed,¹ and the reactive oxygen species (ROS) will be produced when light irradiation works on photosensitizers (PSs) and induces cytotoxicity.² There are 3 mechanisms of PDT: (1) PDT can direct cell killing; (2) PDT can devastate the vasculature; and (3) PDT can initiate immune response. Photodynamic therapy can extend the survival and improve the quality of life for patients with inoperable cancers.³⁻⁵ Photodynamic therapy includes 3 essential elements: PS, light, and reactive oxygen.^{6,7}

Anthraquinone derivative, aloe-emodin (AE), is similar to hypericin in structure.^{8,9} Previous studies had found that AE had anticancer capacity in high concentration alone, such as 10 μM concentration.¹⁰ Aloe-emodin displayed stronger anticancer effect than 5-aminolevulinic acid as a new PS.¹¹

Angiogenesis plays more and more important role in cancer metastasis.¹² Angiogenic factors attract endothelial cells and promote their proliferation. Proliferating and secreting proteases can induce endothelial cells to form blood vessels and enable them to migrate toward the tumor site by breaking open the blood vessels. Proliferating endothelial cells then form new capillary tubes. Finally, the capillaries provide a continuous blood flow for tumor cell metabolism and set up escaping avenues for metastatic tumor cells.¹³⁻¹⁶

The mitogen-activated protein kinase (MAPK) is a type of serine/threonine protein kinase.^{17,18} Mitogen-activated protein kinase can be activated by growth factors, insulin, environmental factors, and cytokines, which involved in a broad intracellular response by the MAPK signaling pathway.^{19,20} Studies found that MAPKs are involved in cell migration and invasion events partially.²¹⁻²³

In this study, AE-PDT induced cell apoptosis and inhibited the proliferation, angiogenesis, migration, and invasion in human umbilical vein endothelial cells (HUVECs). At the same time, we found that AE-PDT can induce apoptosis of HUVECs by activating MAPK signaling pathway.

Materials and Method

Cells

Human umbilical vein endothelial cells (Shanghai Institute of Cell Biology, Shanghai, China) were cultured in Dulbecco's modified Eagle's medium (DMEM) medium (Hyclone, Logan, Utah) supplemented with 10% (vol/vol) fetal bovine serum (Bioind, Hyclone, Logan, Utah), 50 U/mL penicillin, and 50 $\mu\text{g}/\text{mL}$ streptomycin (Hyclone, Logan, Utah) at 5% CO_2 atmosphere and 37°C. Cells in the logarithmic growth phase were harvested for experiments.

Photosensitizer

Aloe-emodin (Jiangxi Herb Fine Co Ltd, Jiang Xi, China; purity >98%) was dissolved in dimethyl sulfoxide (Sigma-Aldrich,

St Louis, Missouri) to prepare stock solution (100 mmol/L). The solutions were sterilized by filtration with a 0.22- μm membrane (Millipore, Bedford, Massachusetts) and stored at -20°C. The stock solution was diluted with DMEM medium (Hyclone) to the desired concentration.

Photodynamic Treatment

Four treatment groups were created: control, single AE, single light, and AE-PDT groups. Cells and AEs were cocultured for 6 hours and then washed 2 times by phosphate-buffered saline (PBS). Irradiations were performed using a blue LED device (430 nm) with a fluence rate of 40 mW/cm^2 ; by adjusting the exposure time, the total light energy was 4, 8, 12, or 16 J/cm^2 : total light dose (J/cm^2) = fluence rate (mW/cm^2) \times treatment time (seconds). Cells were maintained in complete medium during and posttreatment before assays.

Cell Viability

The viability of HUVECs was detected with the WST-8 assay (WST-8 Cell Proliferation Assay Kit, Dojindo, Japan). Absorbance was measured at 450 nm (Tecan Group Ltd, Mannedorf, Switzerland), and the percentage of survival cell was calculated.

5-Ethynyl-2-Deoxyuridine Assay

Cells were incubated with 50 μM 5-ethynyl-2-deoxyuridine (EdU labeling/detection kit; Ribobio, Guangzhou, China) for 12 hours and fixed with 4% paraformaldehyde (PA; pH 7.4) for 30 minutes. Cells were incubated with glycine for 5 minutes. Then anti-EdU solution was added into cells at room temperature and stored for 30 minutes after which cells were washed in PBS containing 0.5% Triton X-100. Finally, 5 $\mu\text{g}/\text{mL}$ Hoechst 33342 was added to the cells and incubated for 30 minutes at room temperature to stain cellular nuclei and observed under a fluorescence microscope (Nikon, Japan).

Tube Formation Assay

Subconfluent HUVECs were harvested, resuspended in medium, and treated with AE-PDT. This suspension was seeded (70 000 cells/well) in Matrigel (Becton Dickinson, San Jose, California; Matrigel:free medium = 1:1) in a 96-well plate and incubated for 24 hours at 37°C with 5% CO_2 . Tube formation was examined under an inverted microscope and photographed at 40 \times magnification. Cumulative tube length was measured by using ImageJ software.²⁴ Results were shown as the mean and standard errors of triplicate experiments.²⁵

Detection of ROS

Cells were cocultured with 2,7-dichlorodihydrofluorescein diacetate (DCFH-DA) (Invitrogen, Paisley, United Kingdom) in a concentration of 10 μM for 30 minutes and washed twice with PBS. Then, the intracellular ROS were analyzed under

fluorescence microscope (Nikon) and Fluor spectrophotometer (Tecan Group Ltd; Excitation = 488 nm, Emission = 520 nm).

Assay for Apoptosis

Cells treated with AE-PDT were resuspended with 500 μ L binding buffer and then incubated with annexin fluorescein Isothiocyanate (V-FITC) and Propidium dioxide (PI) in a Ca^{2+} -enriched binding buffer for 5 minutes. FACS Canto flow cytometer (Becton Dickinson) was used to determine whether the cellular death pathway was apoptotic or necrotic.

Mitochondrial Membrane Potential

5,5',6,6'-tetrachloro-1,1',3,3'-tetraethylbenzimidazolcarbocyanine iodide (JC-1) assay was performed to detect the mitochondrial membrane potential. Cells were incubated with 5 μ g/mL of JC-1 (Invitrogen) for 30 minutes. Then, the membrane potential was measured in Spectra Fluor spectrophotometer (Tecan Group Ltd) and fluorescence microscopy (Nikon).

Western Blot Analysis

Cells were harvested and lysated with radio-Immunoprecipitation (RIPA) buffer (Sigma). Lysates were separated by sodium dodecyl sulfate polyacrylamide gel electrophoresis and then transferred to nitrocellulose membranes (Millipore). Blots were incubated with primary antibodies and secondary antibodies. Antibodies used in this study included Bcl-2, caspase-9, matrix metalloproteinase (MMP) 2, and MMP9, from Santa Cruz Biotechnology (Dallas, Texas); P-38, extracellular signal-regulated kinase (ERK), the c-Jun N-terminal kinases (JNK), and vascular endothelial growth factor (VEGF) from Abcam (Cambridge, Massachusetts); and caspase-3 and glyceraldehyde-3-phosphate dehydrogenase (GAPDH) from Cell Signaling Technologies. The blots were developed by an enhanced chemiluminescence (ECL) detection kit (Kaiji Bio Co, Nanjing, China) and visualized under LAS 3000 Luminoimage Analyzer. Three independent experiments were performed, and the representative results were shown.

Cell Migration and Invasion

The migration or invasive ability of cells was detected by Transwell chamber system (10-mm diameter of polycarbonate membrane with 8-mm pore size; Corning Costar, Cambridge, Massachusetts) coated with or without Matrigel (Becton Dickinson). Briefly, 50 μ L Matrigel (Matrigel:free medium = 1:3) was added into transwell chambers and incubated at 37°C overnight. After fixation in 4% PA (Nanjing Sunshine Biotechnology Ltd, Nanjing, China), the cells invading through the membrane were stained with crystal violet (Nanjing Sunshine Biotechnology Ltd). The migratory and invasive cells were counted by microscope.

Subcellular Localization of AE

During the last 30 minutes of AE incubation, cells were coloaded with Mito-Tracker green at a final concentration of 500 nM to tag the mitochondria. An overlapped fluorescence from organelle probe and AE was observed under confocal microscopy (TCS SP5; Leica).

Cytoskeleton

Cells were seeded into a 96-well plate at a density of 1×10^5 /mL for 24 hours and fixed with 4% PA (Nanjing Sunshine Biotechnology Ltd) for 10 minutes. Cells were permeabilized in PBS containing 0.5% Triton X-100 for 10 minutes, stained with Alexa Fluor 488 phalloidin (Life technologies) for 1 hour, and mounted by microscope.

Transmission Electron Microscopy

Cells were fixed in 0.1 M cacodylate buffer containing 2.5% glutaraldehyde for 2 hours at 4°C, followed by a second fixation in 0.1 M cacodylate buffer containing 1% osmium tetroxide for 1 hour at 4°C. After 3 washes in distilled H₂O, the sample was stained with 0.5% aqueous uranyl acetate for 2 hours at room temperature. Transmission electron microscopy samples were observed using a JEOL1200EX instrument.

Statistical Analysis

Values were expressed as mean (standard deviation). The significance of differences between treatment groups was performed with analysis of variance test or 2-tailed Student *t* test. A value of $P < .05$ was considered statistically significant.

Results

Aloe-Emodin PDT-Suppressed Cell Proliferation

Treatment groups consisted of control, single AE, single light, and AE-PDT groups. Figure 1 shows changes in cell viability caused by different treatments. Aloe-emodin alone with a concentration of 20 μ M and light irradiation alone with a density not less than 16 J/cm² significantly decreased the cell survival ($P < .05$; Figure 1A). Thus, the concentration of AE was set at 15 μ M, and the density of light irradiation was set at 12 J/cm² in the following experiments of AE-PDT, which led to a cell survival rate of 56%. The population of EdU-positive cells was 35 ± 3 , 34 ± 4 , 32 ± 3 , and 8 ± 2 in control, single AE, single light, and AE-PDT groups, respectively. The EdU-positive cells significantly declined in the AE-PDT group compared to the other 3 groups ($P < .05$; Figure 1B and C). No significant differences were observed among the control, single AE, and single light groups ($P > .05$).

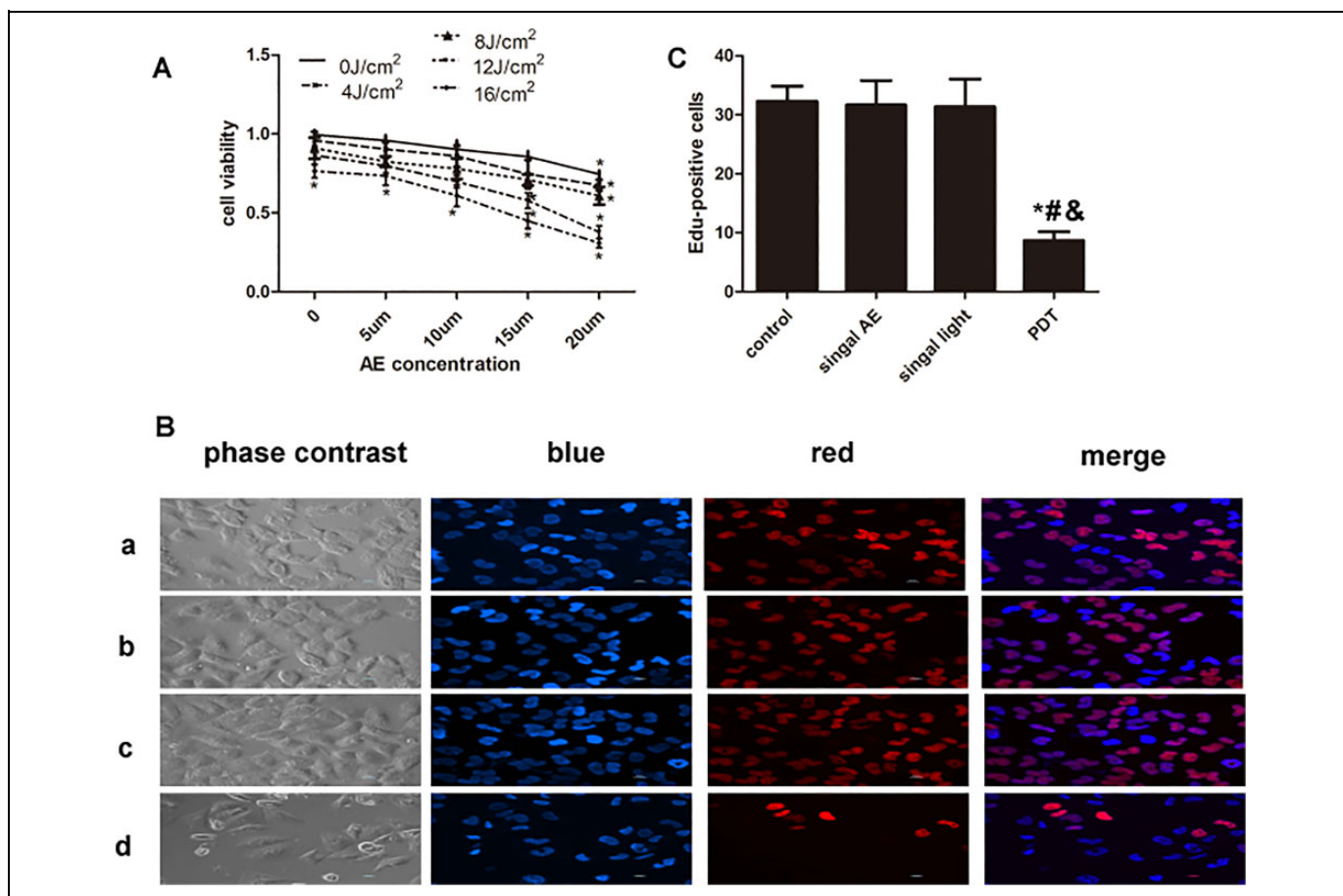


Figure 1. Aloe-emodin photodynamic therapy (AE-PDT) produced cytotoxicity and inhibited proliferation of human umbilical vein endothelial cells (HUVECs). A, The viability of cells was detected by the WST-8 assay. B, The expression of 5-ethynyl-2-deoxyuridine (EdU) was detected by immunofluorescence, and morphology was observed by phase-contrast visualization (EdU, $\times 400$); EdU (red) and H-33342 (blue) staining of DNA. (a) Control group, (b) single AE group, (c) single light group, and (d) AE-PDT group. C, The number of EdU-positive cells. *The AE-PDT group versus control group, $P < .05$. #The AE-PDT group versus single AE group, $P < .05$. &The AE-PDT group versus single light group, $P < .05$. Values were represented as mean (standard deviation [SD]) of 3 independent determinations.

Aloe-Emodin PDT-Induced Apoptosis via the Mitochondria Pathway

Annexin V/PI staining demonstrated a significantly higher apoptotic percentage of death cells in the AE-PDT group ($P < .05$), with a value of 28.8%. No significant differences were observed among the other 3 groups ($P > .05$; Figure 2A and B). JC-1 staining demonstrated that a significant decrease in mitochondrial membrane potential was observed in the AE-PDT group ($P < .05$), whereas no significant differences were observed among the other 3 groups ($P > .05$; Figure 2C and D). Furthermore, the ratio of green to red fluorescence in the AE-PDT group increased to 2.3 times when compared to the control group. It is suggested that AE-PDT induces apoptotic cell death in HUVEC cells via the mitochondria pathway.

Subcellular Localization of AE

Mito-tracker was used to view the subcellular localization of AE in the HUVECs. Overlapping regions (yellow) were

regarded as the subcellular localization of AE. The results showed that the fluorescence images of the mitochondria probe were partially overlapping with the AE (Figure 3).

The Expression of Caspase-9 and Caspase-3

The Western blot results showed that the expression of both caspase-9 and caspase-3 was significantly amplified after AE-PDT ($P < .05$; Figure 4). These data also suggest that AE-PDT induces apoptosis through the mitochondria pathway.

Aloe-Emodin PDT Suppressed Cell Migration and Invasion

The average count of migratory cells in the AE-PDT group was 72 and significantly decreased, while the one in the control, single AE, and single light groups were 288, 286, and 282, respectively. The average number of invasive cells in the AE-PDT group was 19 and significantly declined when

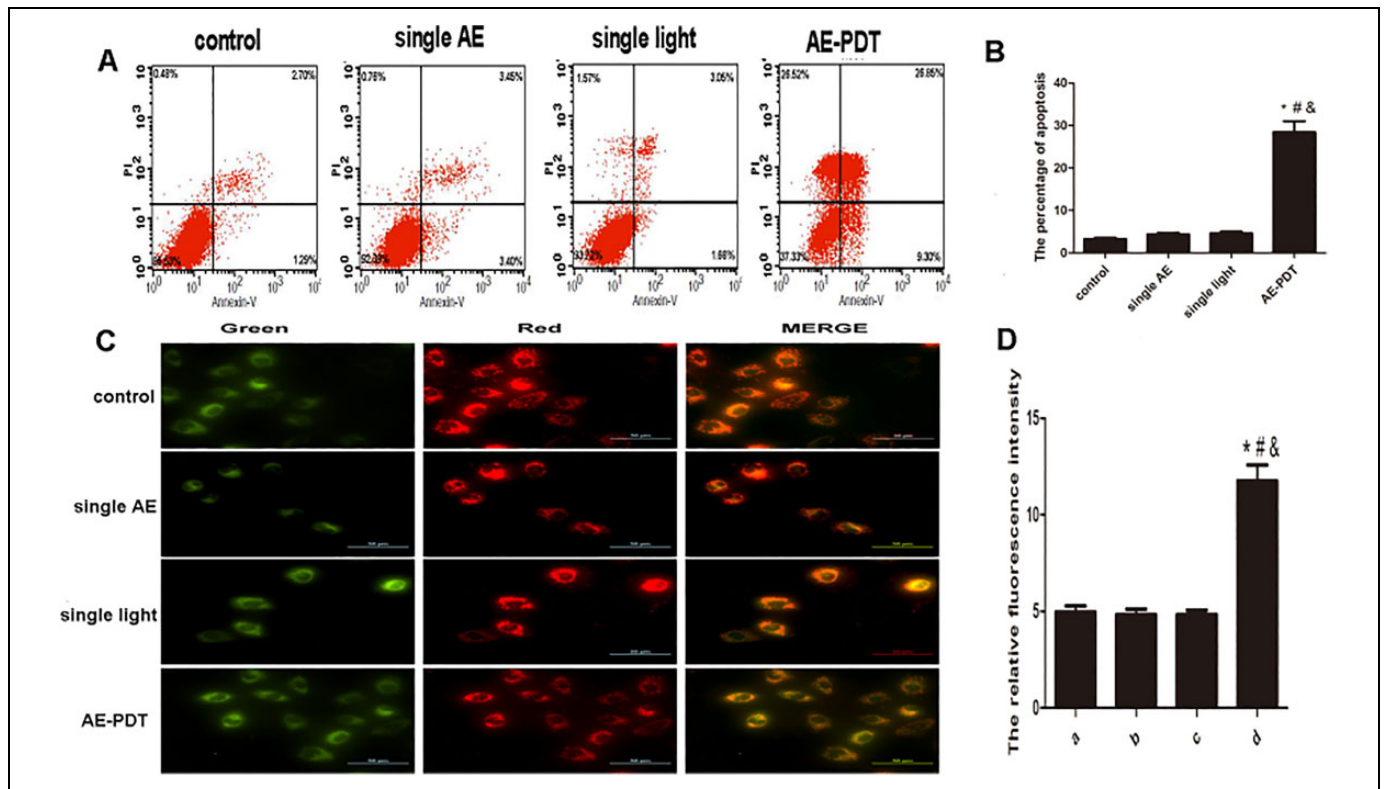


Figure 2. A, Apoptosis detected by annexin V/PI double staining. B, The percentage of apoptosis. C, Mitochondrial membrane potential detected by the JC-1 assay ($\times 200$). D, The relative fluorescence intensity of mitochondrial membrane potential quantified by Fluor spectrophotometer. Scale bar was 50 μm . *Aloe-emodin photodynamic therapy (AE-PDT) group versus control group, $P < .05$. #The AE-PDT group versus single AE group, $P < .05$. &The AE-PDT group versus single light group, $P < .05$. Values were represented as mean (standard deviation [SD]) of 3 independent experiments.

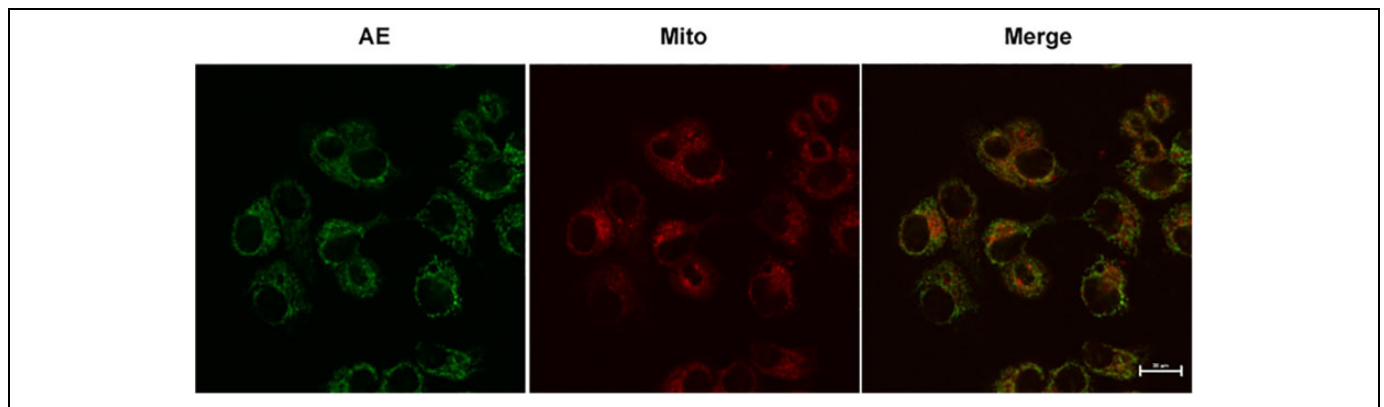


Figure 3. Subcellular localization of aloe-emodin (AE) detected by confocal microscopy. Red fluorescent corresponds to AE, while green fluorescent shows Mito-Tracker with which shows the mitochondrion is stained. Yellow fluorescent indicates colocalization of red and green fluorescence.

compared to the control, single AE, or single light groups, with values of 98, 93, and 92, respectively ($P < .05$; Figure 5A-C).

Cytoskeleton Associated With Migration

Based on the data in cell migration, the effect of PDT on F-actin was explored using TRITC-phalloidin. F-actin in the AE-PDT group was shorter than that in the control, single AE,

or single light groups, demonstrating a reduction in stress and the formation of aggregates (Figure 6).

Aloe-Emodin PDT Negatively Regulates Angiogenesis

Matrigel tubule formation assay was used as an *in vitro* model to study the effect of AE-PDT on the capillary structure formation. As shown in Figure 7A, AE-PDT-treated cells reduced

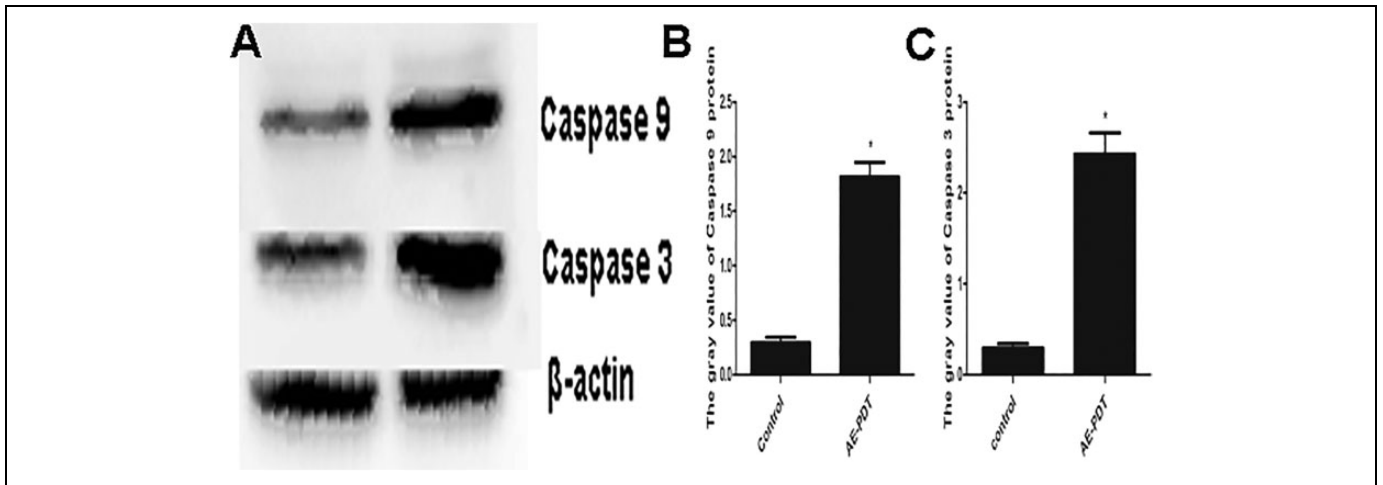


Figure 4. A, Expression of caspase-9 and caspase-3. B-C, Quantitative analysis of protein expression according to panels. The vertical axis represents the gray value of caspase-9 and caspase-3. Each assay condition was done in triplicate. Data were represented as means (standard deviation [SD]).

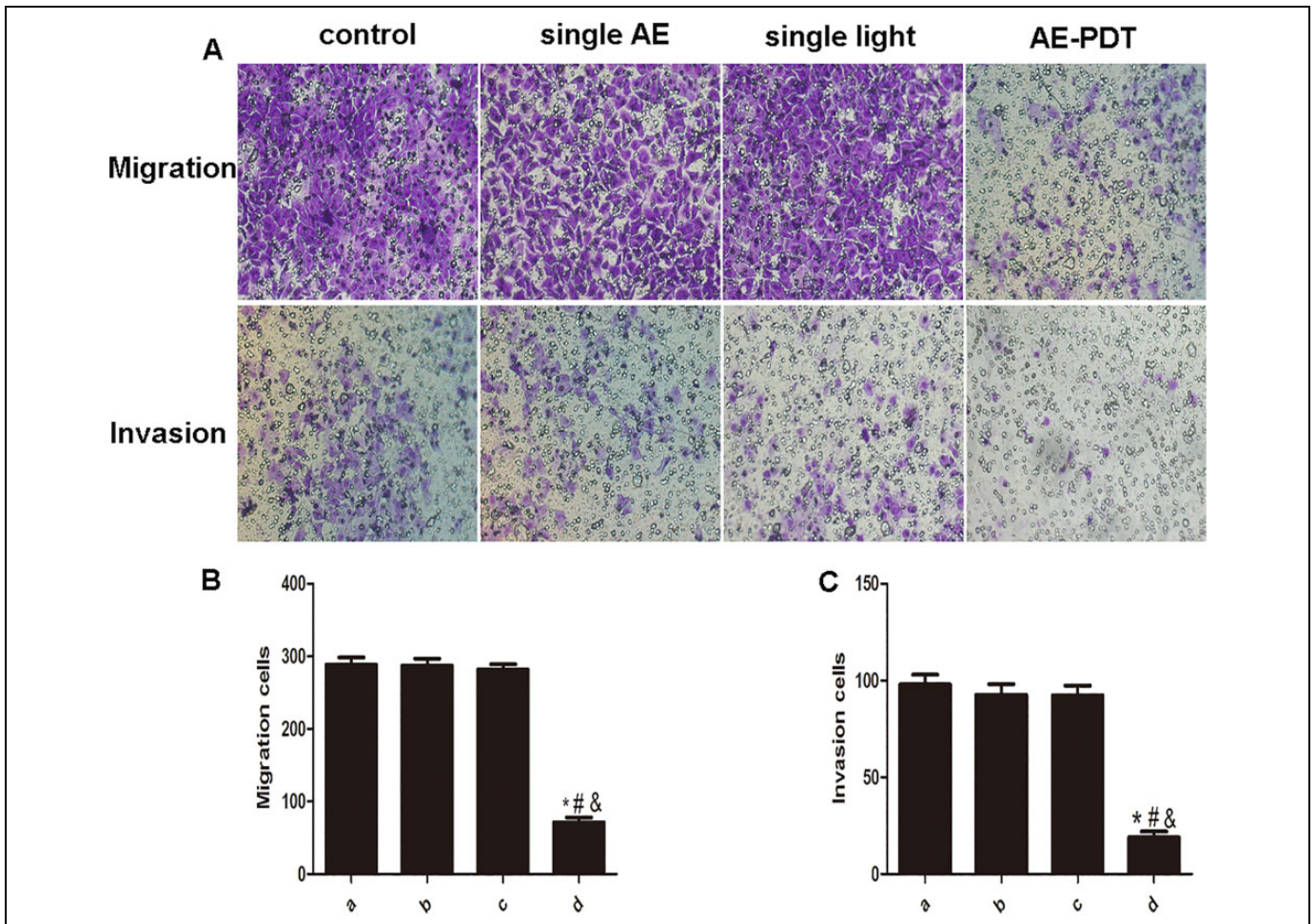


Figure 5. Aloe-emodin photodynamic therapy (AE-PDT) inhibited the migration and invasion of human umbilical vein endothelial cells (HUVECs). A, The AE-PDT suppressed cell migration and invasion. The migration cells and invasion cells were stained by crystal violet (up; crystal violet, $\times 100$). B, The AE-PDT inhibited cell migration. C, The AE-PDT inhibited cell invasion. (a) Control group, (b) single AE group, (c) single light group, (d) AE-PDT group. *The AE-PDT group versus control group, $P < .05$. #The AE-PDT group versus single AE group, $P < .05$. &The AE-PDT group versus single light group, $P < .05$. Each assay condition was done in triplicate. Data were represented as means (standard deviation [SD]).

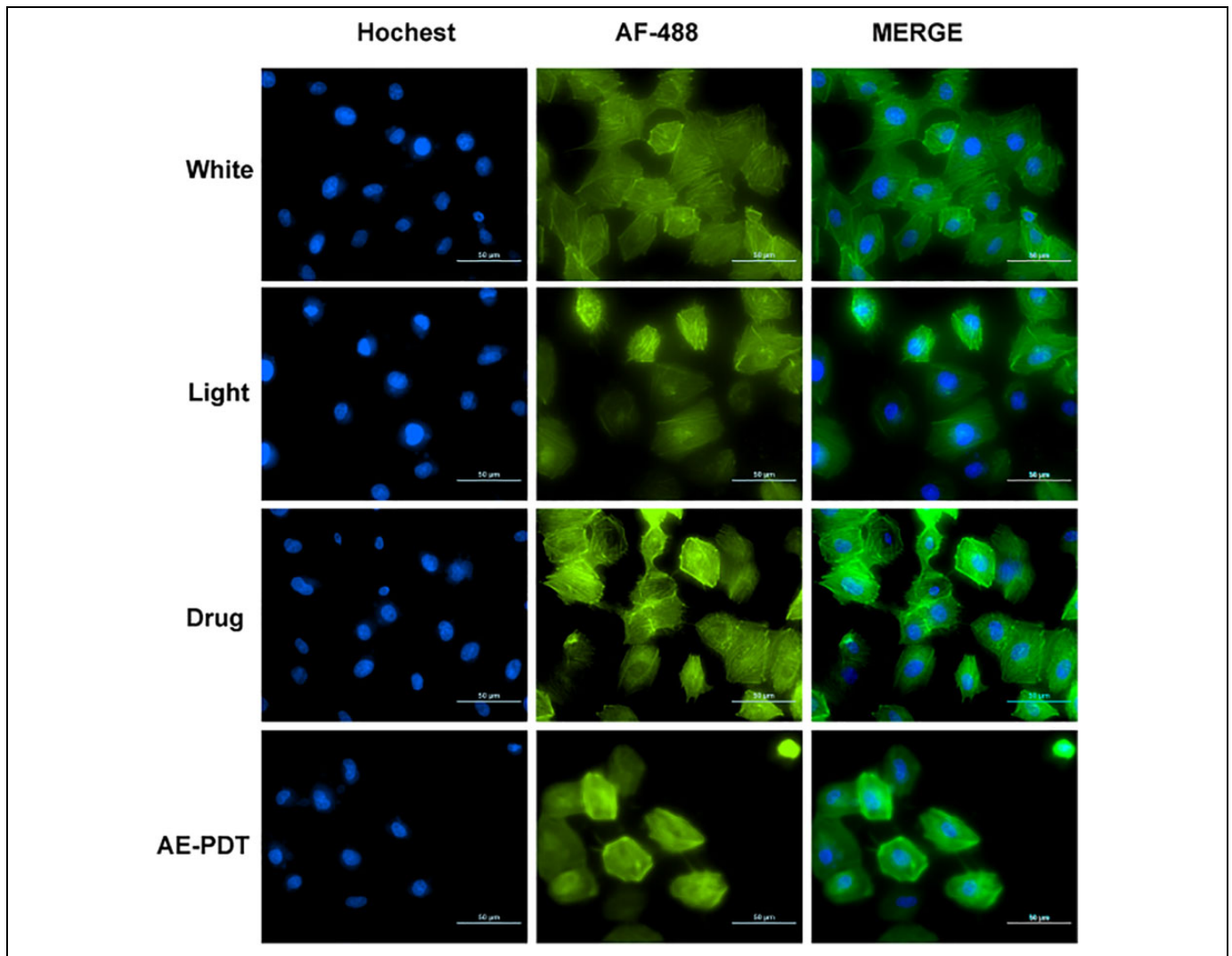


Figure 6. Cytoskeleton associated with migration F-actin(green) was detected by Phalloidin-TRITC. DNA(blue) was observed by Hochest-33342. Both were merged in HUVEC cells.

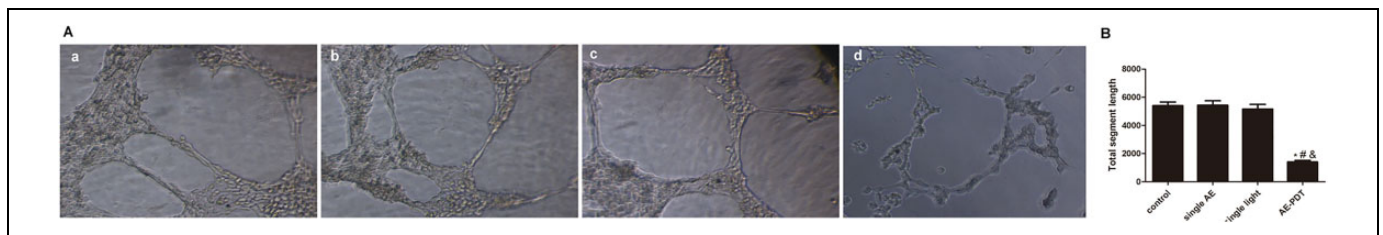


Figure 7. A, The effect of Aloe-emodin photodynamic therapy (AE-PDT) on the capillary structure formation was measured by using Matrigel tubule formation assay. (a) Control group, (b) Single AE group, (c) Single light group, (d) AE-PDT group. B, The numbers of formed capillary tubes in 4 groups were counted. *The AE-PDT group versus control group, $P < .05$. #The AE-PDT group versus single AE group, $P < .05$. &The AE-PDT group versus single light group, $P < .05$. Values were represented as means (standard deviation [SD]) of 3 independent determinations.

branching points, tubule number, and length. Simultaneously, the number of HUVEC capillary structures was significantly decreased by AE-PDT treatment ($P < .05$; Figure 7B). Taken together, these results indicate that AE-PDT may directly regulate angiogenesis *in vitro*.

Mechanism of AE-PDT in Cell Deactivation Level of ROS

Reactive oxygen species mediates damages to mitochondria, thereby inducing apoptosis.¹⁷ DCFH-DA staining showed that more ROS was significantly produced in the AE-PDT groups

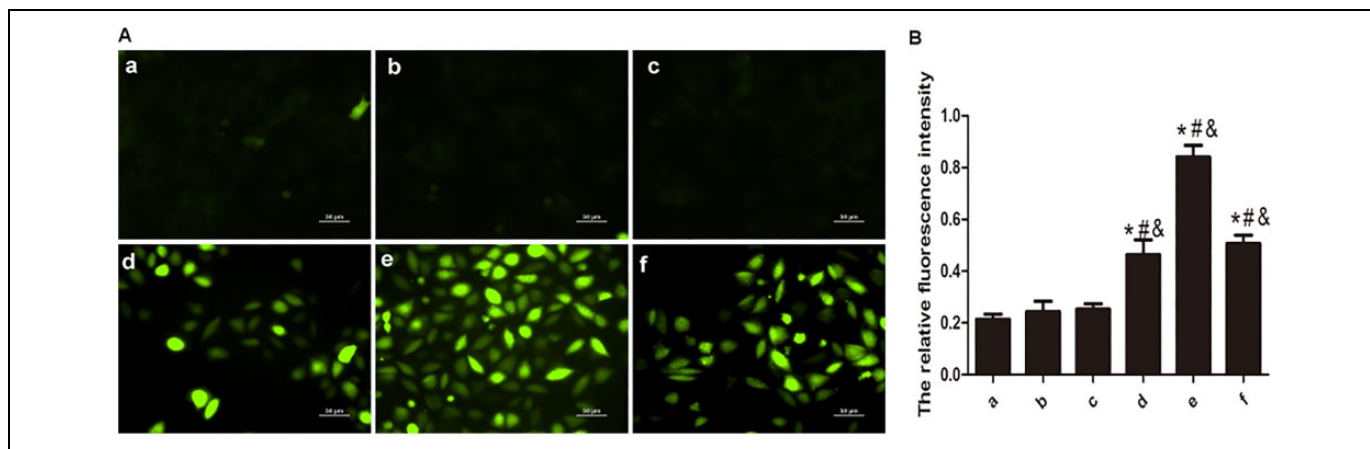


Figure 8. A, Reactive oxygen species (ROS) observed by DCFH-DA staining (DCFH-DA, $\times 200$). DCFH-DA is a nonfluorescent compound, but it can be hydrolyzed and then transferred to DCF, which is highly fluorescent when cells generate ROS. B, Levels of ROS at 30 minutes, 1 hour, and 1.5 hours after aloe-emodin photodynamic therapy (AE-PDT), detected by Fluor spectrophotometer. (a) Control group, (b) Single AE group, (c) Single light group, (d-f): AE-PDT group 30 minutes, 1 hour, and 1.5 hours. *The AE-PDT group versus control group, $P < .05$. #The AE-PDT group versus single AE group, $P < .05$. &The AE-PDT group versus single light group, $P < .05$. Values were represented as means (standard deviation [SD]) of 3 independent determinations.

compared to the other 3 groups ($P < .05$; Figure 8B). The increase in ROS can be detected at 30 minutes and reached the peak at 1 hour after AE-PDT (Figure 8A and B). The data suggest that AE-PDT generates ROS resulting in apoptosis.

The Expression of p38, p-p38, ERK, p-ERK, JNK, p-JNK, and VEGF

Compared to the other 3 groups, the expression of p-p38 and p-ERK ascended, while the expression of VEGF descended significantly in the AE-PDT group ($P < .05$). However, no significant difference was found in the expression of p-JNK among the 4 groups ($P > .05$; Figure 9). These data suggest that MAPK signaling pathways are possibly involved in the inhibition of metastasis of HUVECs induced by AE-PDT.

Discussion

Our data suggest that AE-PDT can inhibit cell proliferation, migration, invasion, and angiogenesis and induce apoptosis. We also delineated the mechanisms. On the one hand, ROS generated by AE-PDT triggers the HUVEC apoptosis through the mitochondria. On the other hand, MAPK signaling pathways triggered by ROS may be involved in the inhibition of angiogenesis, migration, and invasion in HUVEC induced by AE-PDT.

Photodynamic therapy has advantages such as minimal toxicity to normal tissues and lack of intrinsic or acquired resistance.³ In general, the cardinal principium of PDT is that the PS is activated to generate ROS and their derivatives. Then, cellular oxidative stress, tissue anoxia, vasculature damage, and immune response are followed, which result in cell death.²⁶ An ideal PS, which plays a key role in PDT, should be ease of quality control, low costs as well as good stability, and have a high absorbance coefficient at 400 to 800 nm (blue to deep red).

Aloe-emodin is such a novel compound, and the effects of AE-PDT require investigation.

Data in cytotoxic and EdU assays showed that AE-PDT suppressed cell proliferation. Annexin V/PI staining demonstrated a higher percentage of apoptotic cells in group AE-PDT. The apoptosis pathway was therefore explored. Given the short life and limited diffusion distance of AE in biological systems (half-life < 0.04 microseconds and acting radius of action < 0.02 μm), the primary site of photodamage coincides with the intracellular localization of AE.²⁷ Thus, we detected the subcellular localization of AE. Our data suggested that AE was localized mainly on the mitochondrion in HUVECs, which provoked us to seek the further events of mitochondrion. Interestingly, JC-1 staining showed a decrease in mitochondrial membrane potential in the AE-PDT group (Figure 2C-D). It is well known that, first the collapse of mitochondrial membrane potential recruits procaspase-9 to form a multimeric protein complex, subsequently the autoproteolytic activation of caspase-9 is followed, and then the activation of downstream of caspase-3 is initiated to complete the apoptosis process.²⁸⁻³⁰ The collapse of mitochondrial membrane potential as well as increase in caspase-9 and caspase-3 found after AE-PDT in the present study demonstrates that AE-PDT induces apoptosis via the mitochondria pathways.

In the present study, the capacity of HUVEC migration and invasion was suppressed by AE-PDT treatment. Moreover, F-actin, a key factor involved in cell proliferation and migration, was also inhibited by the treatment of AE-PDT. It is now well established that migration and invasion take part in the metastasis³¹; simultaneously, the process of angiogenesis is essential to the growth of both primary and metastatic tumors.³² Besides the inhibition of migration and invasion in HUVECs shown in the present study, the Matrigel tubule formation assay and the expression of VEGF demonstrated that the angiogenesis of HUVECs was also suppressed by AE-PDT.

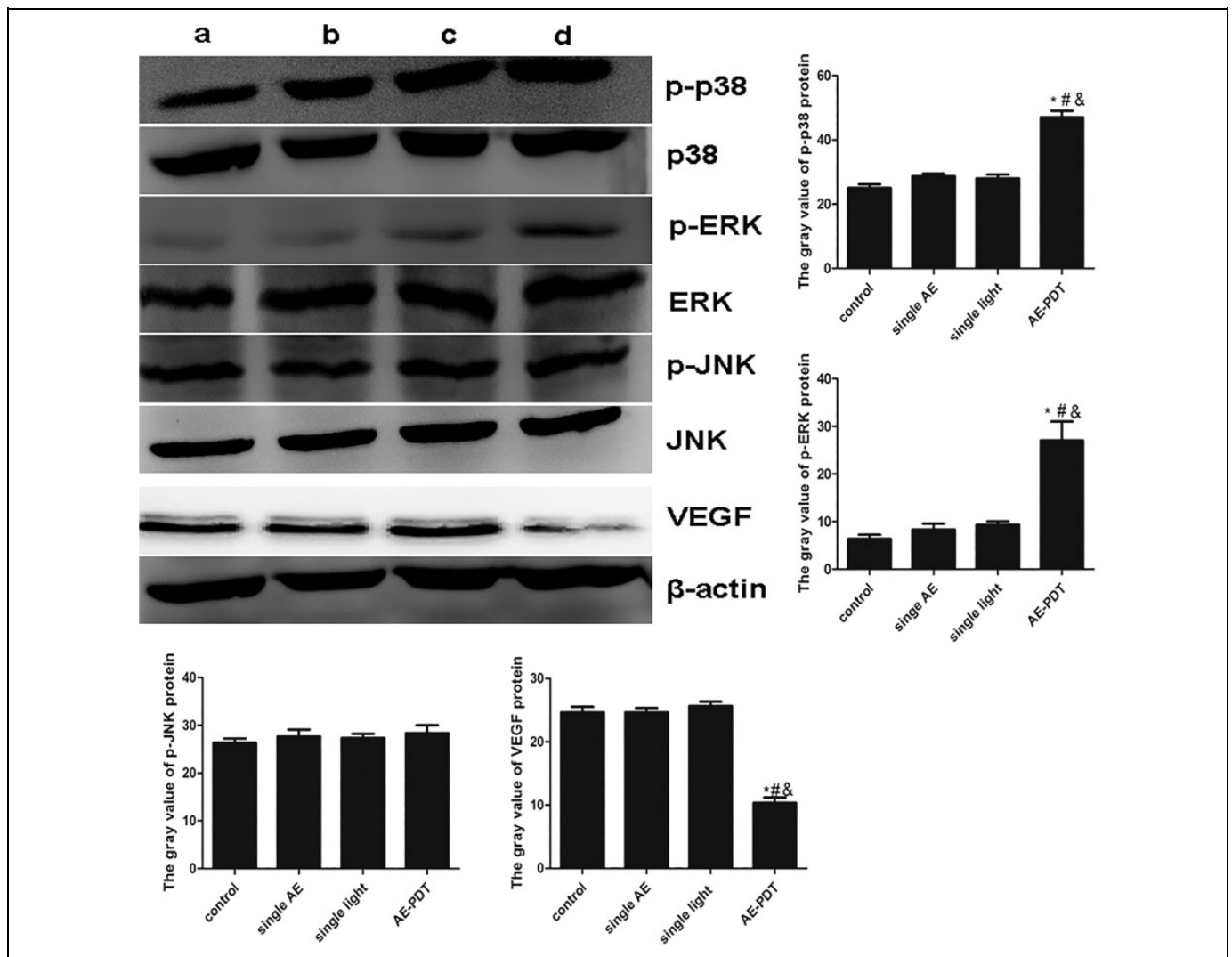


Figure 9. The expression of p38, p-p38, ERK, p-ERK, JNK, p-JNK and VEGF. a: control, b: single AE group, c: single light group, d: AE-PDT group.

It has been found that many factors, including positive and negative ones, take part in the angiogenesis and metastasis.^{33,34} The MAPK pathway has been demonstrated to serve a critical role in the angiogenesis and metastasis,^{35,36} which provoked us to explore the change in MAPK pathway. The MAPK family consists of the 3 kinases: the ERK, the stress-activated protein kinase/JNK, and p38. The activity and the role of the MAPKs have, to some extent, been studied after PDT and are suspected to be of importance in the cellular processes controlling death and survival after oxidative stress.^{37,38} Study showed that the p38 activation serves as a death signal, the JNK activation serves as a rescue signal, whereas the ERK activation has no influence on the treatment outcome.³⁹ Interestingly, our study showed that the expression of p-p38 and p-ERK ascended, while the expression of p-JNK did not change after AE-PDT. Otherwise, the link between MAPK pathway and cell angiogenesis as well as metastasis in colorectal cancer is well established.²³ It was indicated that activation of the Ras/Raf/MEK/

ERK pathway was involved in the regulation of VEGF (which is important in angiogenesis) in human colorectal cancer.²¹ Similarly, interactions between the cell surface urokinase plasminogen activator receptor and integrins are crucial for tumor invasion and metastasis, and urokinase plasminogen activator increases basal ERK activation.²² The reduction in VEGF along with the augment of p-ERK and p-p38 was demonstrated in this study, indicating that both VEGF and ERK, p38 signaling pathways are involved in the suppression of angiogenesis and metastasis in HUVECs. Taken together, these results suggest that AE-PDT inhibits cell proliferation, migration, invasion, and angiogenesis in which the p38 and ERK MAPK signal pathways are involved.

Conclusion

In summary, AE-PDT induced cellular apoptotic cell death via the mitochondria pathways as well as inhibited cell migration,

invasion, and angiogenesis via p38 and ERK MAPK signal pathways.

Acknowledgments

The authors are grateful for the support from Laboratory of Lipid and Glucose Metabolism, the First Affiliated Hospital of Chongqing Medical University, Chongqing, People Republic of China. The authors recognize the valuable contribution of Prof T. H. Yu (Department of Gynaecology and Obstetrics, The Second Affiliated Hospital of Chongqing Medical University, Chongqing, China) and Mr Chen (Flow Cytometry, Centro Nacional de Biotecnología, Madrid).

Declaration of Conflicting Interests

The author(s) declared no potential conflicts of interest with respect to the research, authorship, and/or publication of this article.

Funding

The author(s) disclosed receipt of the following financial support for the research, authorship, and/or publication of this article: This work was supported by the National Natural Science Foundation of China (81101692), National Natural Science Foundation of China (81171859), and Natural Science Foundation Project of CQ CSTC (2011BB5136).

ORCID iD

Ding-Qun Bai, PhD  <http://orcid.org/0000-0002-6727-4634>

References

1. Josefsen LB, Boyle RW. Unique diagnostic and therapeutic roles of porphyrins and phthalocyanines in photodynamic therapy, imaging and theranostics. *Theranostics*. 2012;2(9):916-966.
2. Zhao JF, Wang J, Chen JY, et al. Gallium phthalocyanine photosensitizers: carboxylation enhances the cellular uptake and improves the photodynamic therapy of cancers. *Anticancer Agents Med Chem*. 2012;12(6):604-610.
3. Agostinis P, Berg K, Cengel KA, et al. Photodynamic therapy of cancer: an update. *CA Cancer J Clin*. 2011;61(4):250-281.
4. Peitzu LI, Ensheng KE, Tsuimin T, et al. ALA- or Ce6-PDT induced phenotypic change and suppressed migration in surviving cancer cells. *J Dent Sci*. 2015;1(10):74-80.
5. Allison RR, Moghissi K. Oncologic photodynamic therapy: clinical strategies that modulate mechanisms of action. *Photodiagnosis Photodyn Ther*. 2013;10(4):331-341
6. Dougherty TJ, Gomer CJ, Henderson BW, et al. Photodynamic therapy. *J Nat Cancer Inst*. 1998;90(12):889-905.
7. Acedo P, Stockert JC, Canete M, Villanueva A. Two combined photosensitizers: a goal for more effective photodynamic therapy of cancer. *Cell Death Dis*. 2014;5:e1122.
8. Bais HP, Vepachedu R, Lawrence CB, Stermitz FR, Vivanco JM. Molecular and biochemical characterization of an enzyme responsible for the formation of hypericin in St. John's wort. *J Biol Chem*. 2003;278(34):32413-32422.
9. Zobayed SM, Afreen F, Goto E, Kozai T. Plant-environment interactions: accumulation of hypericin in dark glands of *Hypericum perforatum*. *Ann Bot*. 2006;98(4):793-804.
10. Lee MS, Lee GM. Effect of hypoosmotic pressure on cell growth and antibody production in recombinant Chinese hamster ovary cell culture. *Cytotechnology*. 2001;36(1-3):61-69.
11. Lee HZ, Yang WH, Hour MJ, et al. Photodynamic activity of aloe-emodin induces resensitization of lung cancer cells to anoikis. *Eur J Pharmacol*. 2010;648(1-3):50-58.
12. Harp D, Driss A, Mehrabi S, et al. Exosomes derived from endometriotic stromal cells have enhanced angiogenic effects in vitro. *Cell Tissue Res*. 2016;365(1):187-196.
13. Carmeliet P, Jain RK. Principles and mechanisms of vessel normalization for cancer and other angiogenic diseases. *Nat Rev Drug Discov*. 2011;10(6):417-427.
14. Jain RK. Normalizing tumor microenvironment to treat cancer: bench to bedside to biomarkers. *J Clin Oncol*. 2013;31(17):2205-2218.
15. Goel S, Duda DG, Xu L, et al. Normalization of the vasculature for treatment of cancer and other diseases. *Physiol Rev*. 2011;91(3):1071-1121.
16. Arjaans M, Schröder CP, Oosting SF, Dafni U, Kleibeuker JE, de Vries EG. VEGF pathway targeting agents, vessel normalization and tumor drug uptake: from bench to bedside. *Oncotarget*. 2016;7(16):21247-21258
17. Yoon HE, Oh SH, Kim SA, Yoon JH, Ahn SG. Pheophorbide a-mediated photodynamic therapy induces autophagy and apoptosis via the activation of MAPKs in human skin cancer cells. *Oncol Rep*. 2014;31(1):137-144.
18. Ge X, Liu J, Shi Z, et al. Inhibition of MAPK signaling pathways enhances cell death induced by 5-aminolevulinic acid-photodynamic therapy in skin squamous carcinoma cells. *Eur J Dermatol*. 2016;26(2):164-72.
19. Qiu JW, Guo W, Shen LJ. Advances In research on p38 MAPK-related hepatocellular carcinoma. *World Chin J Digestol*. 2009;16:503-509.
20. Mulholland DJ, Kobayashi N, Ruscetti M, et al. Pten loss and RAS/MAPK activation cooperate to promote EMT and metastasis initiated from prostate cancer stem/progenitor cells. *Cancer Res*. 2012;72(7):1878-1889.
21. Cassano A, Bagalà C, Battelli C, et al. Expression of vascular endothelial growth factor, mitogen-activated protein kinase and p53 in human colorectal cancer. *Anticancer Res*. 2002;22(4):2179-2184.
22. Ahmed N, Oliva K, Wang Y, Quinn M, Rice G. Downregulation of urokinase plasminogen activator receptor expression inhibits Erk signalling with concomitant suppression of invasiveness due to loss of uPARbeta1 integrin complex in colon cancer cells. *Br J Cancer*. 2003;89(2):374-384.
23. Jing YF, Bruce CR. The MAPK signalling pathways and colorectal cancer. *Lancet Oncol*. 2005;6(5):322-327.
24. Schneider DP, Deser C, Okumura Y. An assessment and interpretation of the observed warming of West Antarctica in the austral spring. *Clim Dyn*. 2012;38:323-347.
25. Swift FV, Zeccola B, Bernard J, et al. In the superior court of the state of delware in and for kent county. *C.A. No*. 2010. 15:1-7.
26. Dolmans DE, Fukumura D, Jain RK. Photodynamic therapy for cancer. *Nat Rev Cancer*. 2003;3(5):380-387.

27. Buytaert E, Dewaele M, Agostinis P. Molecular effectors of multiple cell death pathways initiated by photodynamic therapy. *Biochim Biophys Acta*. 2007;1776(1):86-107
28. Yan N, Shi Y. Mechanisms of apoptosis through structural biology. *Annu Rev Cell Dev Biol*. 2005;21:35-56.
29. Lai JC, Lo PC, Ng DK, et al. BAM-SiPc, a novel agent for photodynamic therapy, induces apoptosis in human hepatocarcinoma HepG2 cells by a direct mitochondrial action. *Cancer Biol Ther*. 2006;5(4):413-418.
30. Yoo JO, Ha KS. New insights into the mechanisms for photodynamic therapy-induced cancer cell death. *Int Rev Cel Mol Bio*. 2012;295:139-174.
31. Adibhatla RM, Hatcher JH. Lipid oxidation and peroxidation in CNS health and disease: from molecular mechanisms to therapeutic opportunities. *Antioxid Redox Signaling*. 2010;12(1):125-169.
32. Ellis LM, Fidler IJ. Angiogenesis and Metastasis. *Eur J Cancer*. 1996;14:2451-2460.
33. Moserle L, Casanovas O. Anti-angiogenesis and metastasis: a tumour and stromal cell alliance. *J Intern Med*. 2013;273(2):128-137.
34. Wang R, Zhao N, Li S, et al. MicroRNA-195 suppresses angiogenesis and metastasis of hepatocellular carcinoma by inhibiting the expression of VEGF, VAV2, and CDC42. *Hepatology*. 2013;58(2):642-653.
35. Lynch CC, Crawford HC, Matrisian LM, McDonnell S. Epidermal growth factor upregulates matrix metalloproteinase-7 expression through activation of PEA3 transcription factors. *Int J Oncol*. 2004;24(6):1565-1572.
36. Zhang J, Anastasiadis PZ, Liu Y, Thompson EA, Fields AP. Protein kinase C (PKC) betaII induces cell invasion through a Ras/Mek-, PKC iota/Rac 1-dependent signaling pathway. *J Biol Chem*. 2004;279(21):22118-22123.
37. Almeida RD, Manadas BJ, Carvalho AP, Duarte CB. Intracellular signaling mechanisms in photodynamic therapy. *Biochim Biophys Acta*. 2004;1704(2):59-86.
38. McCubrey JA, Lahair MM, Franklin RA. Reactive oxygen species-induced activation of the MAP kinase signaling pathways. *Antioxid Redox Signal*. 2006;8(9-10):1775-1789.
39. Weyergang A, Kaalhus O, Berg K. Photodynamic therapy with an endocytically located photosensitizer cause a rapid activation of the mitogen-activated protein kinases extracellular signal-regulated kinase, p38, and c-Jun NH2 terminal kinase with opposing effects on cell survival. *Mol Cancer Ther*. 2008;7(6):1740-1750.